Computational study of spin transitions in $BaLiF_3$ containing paramagnetic impurities

2000 J. Phys.: Condens. Matter 12 7243

(http://iopscience.iop.org/0953-8984/12/32/308)

J. Phys.: Condens. Matter **12** (2000) 7243–7254. Printed in the UK PII: S0953-8984(00)12852-8

Computational study of spin transitions in $BaLiF_3$ containing paramagnetic impurities

I Lado-Touriño†§, N Ayad‡, F Tsobnang† and J C Fayet‡

† Institut Supérieur des Matériaux du Mans, 44 Avenue Bartholdi, 72000 Le Mans, France
‡ Laboratoire de Physique de la Matière Condensée, Faculté de Sciences, Université de Maine, Avenue O Messiaen, 72000 Le Mans, France

E-mail: ilado@ismans.univ-lemans.fr

Received 28 March 2000

Abstract. The aim of this work is the computational study of the electronic and magnetic properties of $[FeO_4]^{5-}$ clusters diluted in a cubic host crystal: $BaLiF_3$. Experimental results show that these systems display a bistable magnetic behaviour (intermediate spin $S = 3/2$–high spin $S = 5/2$ transition), which can be reversibly controlled by temperature or light illumination. Our calculations, using density functional theory for both molecular and crystalline models, on two different $[FeO_4]^{5-}$ structures, one with D_{4h} symmetry and another one with C_{2v} symmetry, lead to results that are in good qualitative agreement with experimental results: the structure with D_{4h} symmetry has a quartet ground state and the structure with C_{2v} symmetry has a sextet ground state. The observed spin transition may be understood as a consequence of oxygen jumpings into neighbouring fluorine vacancies in the $BaLiF_3$ matrix under light or thermal excitation, which would allow transformation from one $[FeO_4]^{5-}$ configuration into the other.

1. Introduction

Spin transitions are thermodynamic transitions between spin multiplets of different multiplicity. The first spin transition phenomenon was observed by Cambi and Cagnasso [1] in the 1930s for tri(dithiocarbamate) iron (III) compounds. Since then, extensive studies have been carried out specially on molecular materials based on transition metal ions [2]. Although thermally induced spin transitions are by far the most extensively studied, it was shown experimentally that spin transitions may be also mechanically [3–5] and optically induced [6, 7]. At the microscopic scale the spin transition may be related to intraionic electron transfers between d orbitals with spin flip of the transferred electrons [2].

Up to now, mainly molecular materials based on transition metal ions have been investigated. In a recent work, Ayad [8] observed an intermediate spin–high spin transition induced either by UV light or temperature in $BaLiF_3$ samples obtained from non-purified fluorides using a modified Bridgman method. This spin transition was characterized by means of EPR spectroscopy. Studies on the spin dynamic were also performed. The transition observed involved a spin state $3/2$ with D_{4h} symmetry and a spin state $5/2$ with C_{2v} symmetry. As pure $BaLiF_3$ is a diamagnetic material, the spin transition can be only attributed to impurities. The nature of the latter has yet to be established. According to local symmetry, spin dynamic and thermodynamic analysis, the paramagnetic species proposed by the author is a $[FeO_4]^{5-}$

§ Corresponding author.

0953-8984/00/327243+12$30.00

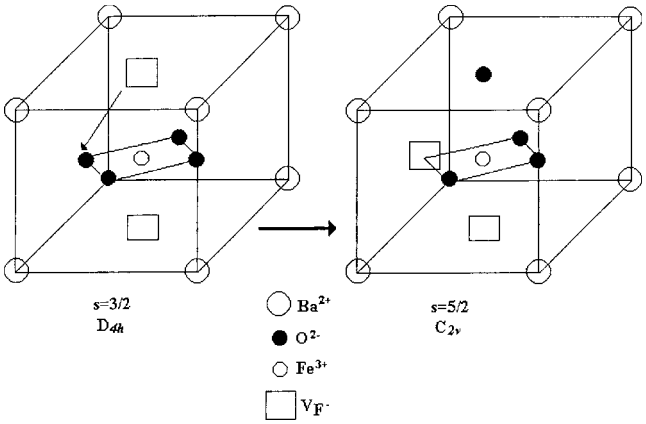

Figure 1. A vacancy displacement allows transformation from configuration D_{4h} into configuration C_{2v}.

complex with D_{4h} ($S = 3/2$) or C_{2v} ($S = 5/2$) symmetry, which occupies an $[LiF_6]^{5-}$ site in the $BaLiF_3$ matrix. Two F^- vacancies ensure local electroneutrality, in such a way that a vacancy displacement would allow transformation from one configuration into the other (figure 1).

The aim of this work is the theoretical study of the electronic and magnetic properties of $[FeO_4]^{5-}$ in a $BaLiF_3$ host lattice. By comparing our results with the experimental ones we tried to confirm the nature of the defect and the origin of its properties. We are particularly interested in the ground state of D_{4h} and C_{2v} $[FeO_4]^{5-}$ clusters and the possibility of optical excitation of the former using UV light in the range 250–350 nm.

2. Experimental background [8]

The elements for the identification of the paramagnetic species and the evidence of the spin transition from EPR measurements can be summarized as follows. Two lines A and B located in the low field part of the EPR spectrum for $H \parallel (100)$ are represented in figure 2. They possess a common feature, narrowness, which rules out a transition element with a nuclear spin surrounded by fluorine atoms at usual metal–ligand distances. Otherwise, well known hyperfine interactions with the metal and ^{19}F nuclei ($I = 1/2$, 100% abundant) should manifest by a substantial broadening or a resolved hyperfine structure. Line A ($g = 4$) belongs unambiguously to a spin $S = 3/2$ with no orbital degeneracy, in a strong quadrupolar spin lattice interaction of tetragonal symmetry along z and parallel to the crystal axes. At X band (10^{10} Hz) this gives the appearance of an effective spin $S^* = 1/2$ with $g_\parallel = 2$ and $g_\perp = 4$. However, the transition $\Delta M_S = -3/2 \rightarrow 3/2$, which is weakly allowed for $H \perp z$, was observed at S band (4×10^9 Hz) and high field (1.2 T). This confirms the existence of a paramagnetic centre with $S = 3/2$. The line related to A for $H \parallel z$ ($g = 2$) is flanked by a weak hyperfine doublet due to ^{57}Fe ($I = 1/2$, 2% abundant). Clear evidence of this doublet (figure 3) could be obtained by saturation of the central line (^{55}Fe, $I = 0$), taking advantage of particular spin relaxation and cross relaxation effects driven by hyperfine interaction with ^{57}Fe. Keeping in mind that the ground state $S = 3/2$ of Fe^{3+} requires a substantial deviation from cubic symmetry, a square plane $[FeO_4]^{5-}$ cluster was suggested to account for the features of line A and related ones.

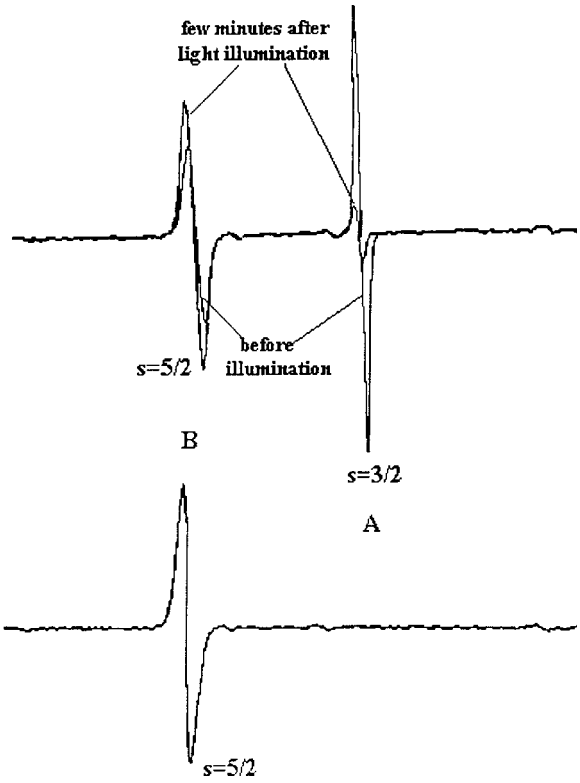

Figure 2. EPR spectra of $BaLiF_3$ samples before and after light illumination.

Line B is only observed at low temperature and is smeared out by dynamic broadening on heating above 250 K. Obviously, it belongs to the fine structure of a spin $S = 5/2$ subjected to an effective crystal field of C_{2v} symmetry with the binary z-axis along (110). An $[FeO_4]^{5-}$ cluster derived from the square plane configuration by the jumping of an O atom into a F^- vacancy can account for the features of line B, provided that the Fe^{3+} system also jumps above the border that separates the spin quartet and the spin sextuplet ground states in the space of the effective crystal field parameters. Illumination at 100 K with UV light induces transformation of A into B and thus, a spin transition $3/2 \rightarrow 5/2$. In the dark, the reverse transition is frozen at low temperature but occurs at an increasing rate on heating above 250 K. Line B is smeared out and the intensity of line A does not follow, by a long way, the Curie law. This is the manifestation of a progressive thermal spin conversion $3/2 \rightarrow 5/2$. On the other hand, an absorption band peaking at 300 nm (4.12 eV) follows the evolution of line A under light and heat treatments (figure 4).

3. Model systems and calculation methods

Two different types of model were used in our calculations:

(i) *Three-dimensional periodic models for the study of pure and $[FeO_4]^{5-}$-doped $BaLiF_3$ (figures 5(A), 5(B) and 5(C)).* Figure 5(A) shows the inverse perovskite structure of $BaLiF_3$ (space group O_h^1—$Pm3m$, lattice parameter $a = 2$ Å), where the monovalent ion is at the centre of an octahedron, whereas the divalent ion is in a 12-fold environment site. Both

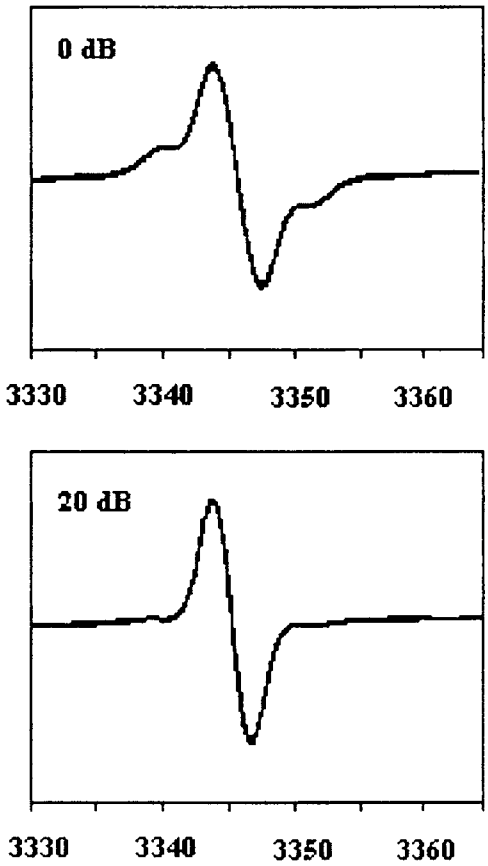

Figure 3. Hyperfine structure due to ^{57}Fe ($I = 1/2$) for $H \parallel z$ ($g = 2$) and saturation effects on the central line (^{55}Fe).

sites show cubic symmetry. Hypothetical crystals $Ba_8Li_7F_{18}FeO_4$ with unit cell ($2a$, $2a$, $2a$), were built by substituting an $[LiF_6]^{5-}$ group by an $[FeO_4]^{5-}$ group with D_{4h} or C_{2v} symmetry with $z \parallel(001)$ or $z \parallel(110)$ (figures 5(B) and 5(C)).

(ii) *Molecular models for the study of the two $[FeO_4]^{5-}$ structures (figures 6(A) and 6(B)).* Structure A, which will be identified as the 'cross-shaped' molecule, is formed by a central Fe atom bonded to four O atoms. The bond distance is 2 Å. The molecular symmetry is D_{4h} and all the atoms are in the same plane. Molecule B ('T-shaped' molecule) is built from molecule A by forcing an O atom to go out of the molecular plane. The final symmetry is C_{2v}. Due to the existence of two pairs of non-equivalent O atoms, these are denoted as O1 and O2. The O2–Fe–O2 bond lies along the x-axis.

The systems were studied within the local spin density approximation (LSDA) [9], whose fundamental equation is

$$\{-1/2\nabla^2 + V_{eff}[(\rho^\alpha), (\rho^\beta)]\}\psi_i^s = \varepsilon_i^s \psi_i^s.$$

In this equation ψ_i^s is the molecular orbital term, $-\nabla^2/2$ is the kinetic energy operator and V_{eff} is an effective electronic potential, which includes an electrostatic term, which is purely classical and contains the electrostatic energy arising from the Coulomb attraction between electrons and nuclei, the repulsion between electrons and the repulsion between nuclei and

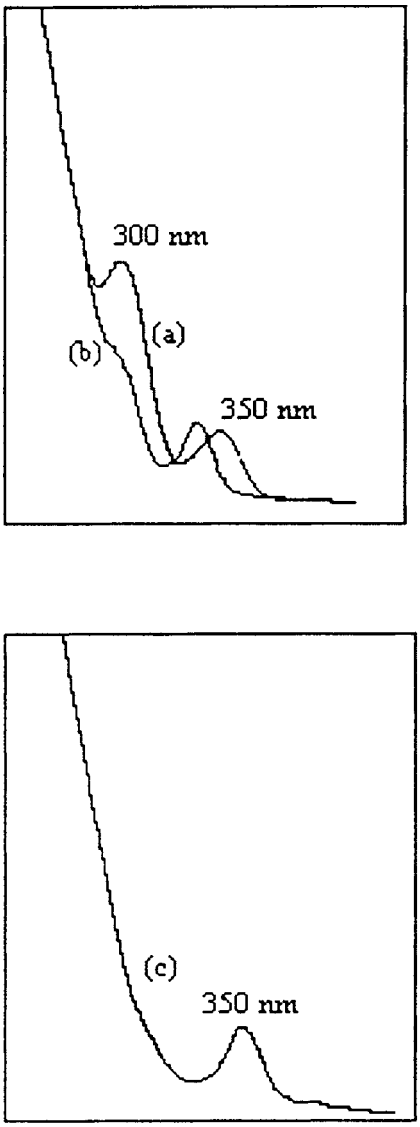

Figure 4. UV–vis spectra under light (a) and (b) and heat treatments (c).

an exchange–correlation term, which describes all remaining electronic contributions. The exchange–correlation term depends on the densities of the electrons with spin α, ρ^{α}, and with spin β, ρ^{β}. The molecular orbitals ψ_i^s and the one-electron energies ε_i^s are different for spin α and spin β electrons, as denoted by the spin label $s = \alpha$ or β.

Calculations on molecular models were performed with the DMol program [10], using the Vosko–Wilk–Nusair exchange–correlation functional [11]. All the calculations were performed with DNP basis (double-numerical basis with polarization functions, that is to say, 3s, 3p, 3d, 4s and 4p atomic orbitals for Fe and 2s, 2p and 3d atomic orbitals for O), frozen inner-core orbitals and a density convergence criterion of 10^{-6} electron/bohr^3 for the energy and electronic density self-consistent field calculations.

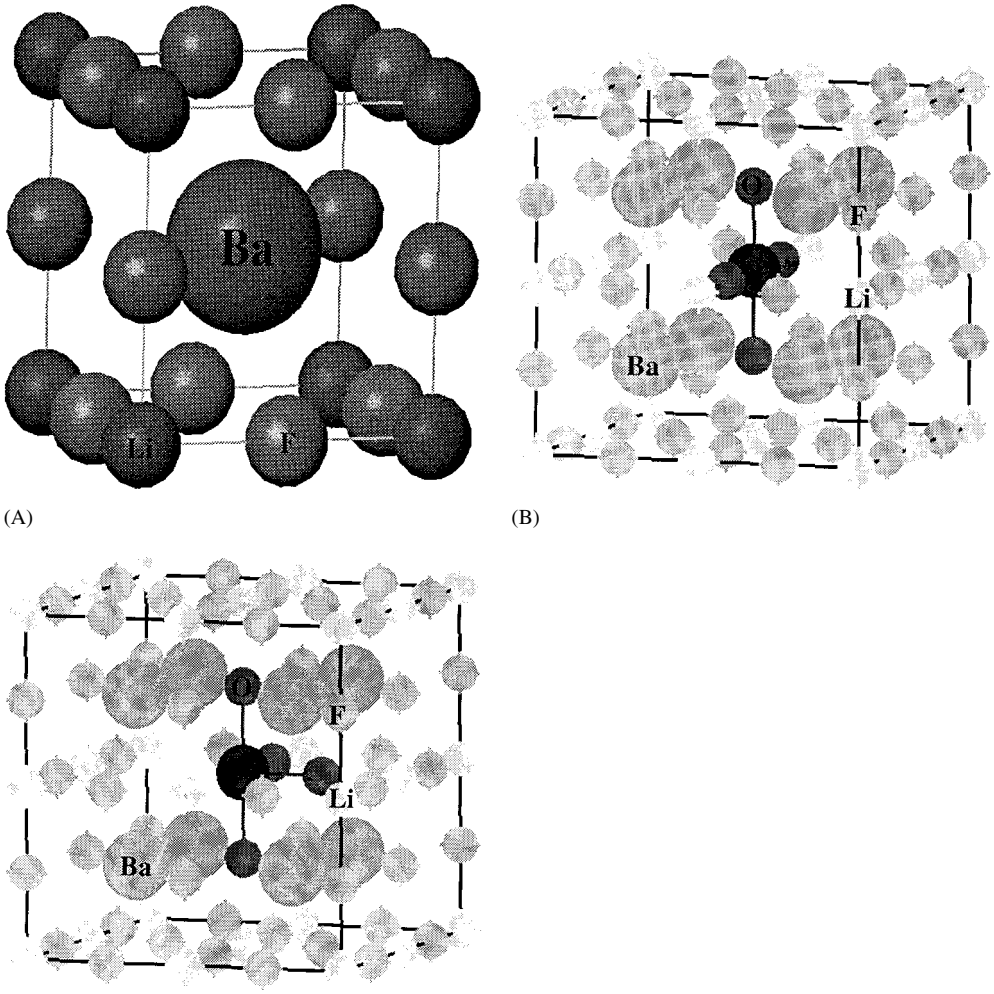

Figure 5. Periodic models for: (A) $BaLiF_3$, (B) cross-shaped $[FeO_4]^{5-}$-doped $BaLiF_3$ and (C) T-shaped $[FeO_4]^{5-}$-doped $BaLiF_3$.

Crystalline models were studied with the ESOCS program [12] within a scalar-relativistic approximation. This program uses a parametrized form of the exchange–correlation energy of the homogeneous electron gas given by Hedin and Lundquist [13] and von Barth and Hedin [14].

4. Results

4.1. Crystalline models

4.1.1. Pure $BaLiF_3$. The band structure calculated for pure $BaLiF_3$ is shown in figure 7. From this figure a band gap of 6.644 eV is obtained. The high electronegativity of fluorine leads to a low energy valence band and a large band gap, typical of an insulator. Our calculations agree with previously reported results [15, 16].

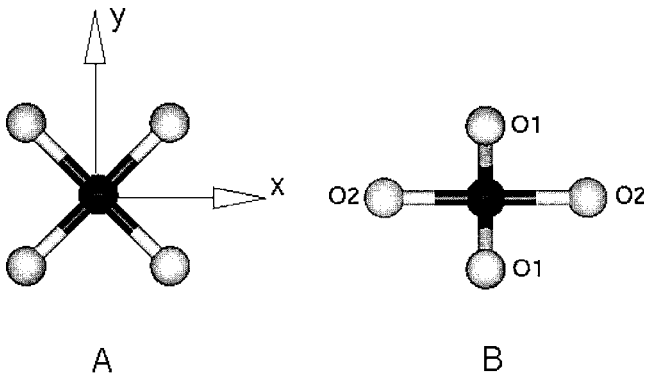

Figure 6. Molecular models for: (A) cross-shaped molecule and (B) T-shaped molecule.

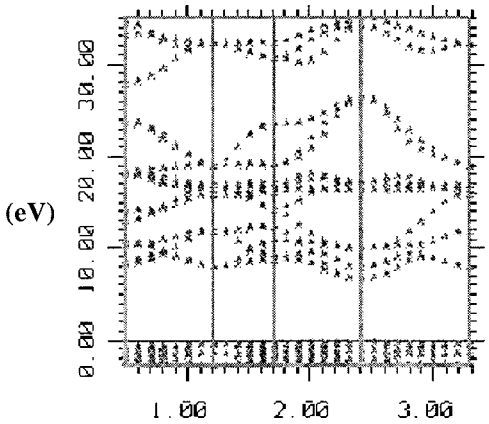

Figure 7. Band structure for pure $BaLiF_3$.

4.1.2. $BaLiF_3$ doped with cross-shaped $[FeO_4]^{5-}$. The band structures for down and up electrons calculated for $BaLiF_3$ doped with cross-shaped $[FeO_4]^{5-}$ are shown in figure 8. One can note the appearance of new energy states in the band gap of pure $BaLiF_3$, which can be attributed to the $[FeO_4]^{5-}$ molecule. The calculated magnetic moment is 2.96 μ_B. The calculated spin populations are 2.57 for the Fe atom and 0.10 for each O atom.

4.1.3. $BaLiF_3$ doped with T-shaped $[FeO_4]^{5-}$. The band structures for down and up electrons are shown in figure 9. Once again, the presence of the $[FeO_4]^{5-}$molecule introduces energy states in the band gap of pure $BaLiF_3$. In this case, the calculated magnetic moment is 4.86 μ_B. The calculated spin populations are 3.27 for the Fe atom, 0.43 for both O1 atoms and 0.24 for both O2 atoms.

4.2. Molecular models

In order to understand the mechanism of magnetic coupling in these structures, we have performed calculations on molecular models with the DMol program. This code allows the calculation of some properties of interest for us, such as spin densities, which cannot be obtained for periodic models with the ESOCS program.

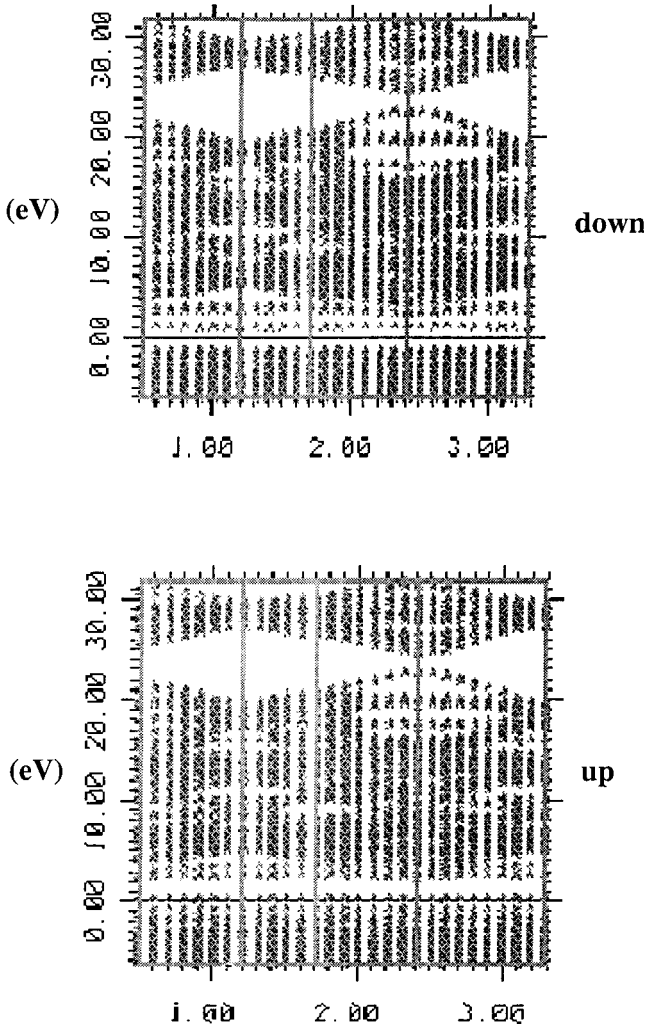

Figure 8. Band structures for cross-shaped $[FeO_4]^{5-}$-doped $BaLiF_3$.

4.2.1. Cross-shaped molecule. The spin value obtained for this molecular geometry is 3/2. In table 1 the α and β spin populations on each atom are shown. The final α spin populations are 2.510 for the Fe atom and 0.123 for each O atom. The initial numbers of electrons in the Fe^{3+} and O^{2-} ions are 23 and 10 respectively. From the values shown in the table, one can see that the Fe^{3+} ion has won 2.604 electrons and each O^{2-} ion has lost 0.651 electrons. The spin density distribution is shown in figure 10. α spin density is represented by the lined surface and β spin density by the black solid surface. A total ferromagnetic coupling between the spin densities located on Fe and O atoms can be observed. Electron charge transfer from the O atoms to the Fe atom accounts for the observed value of $S = 3/2$.

4.2.2. T-shaped molecule. The spin value obtained is 5/2. In table 2 the α and β spin populations on each atom are shown. The final α spin populations are 3.736 for the Fe atom, 0.460 for both O1 atoms and 0.171 for both O2 atoms. In this case, the Fe^{3+} ion has won

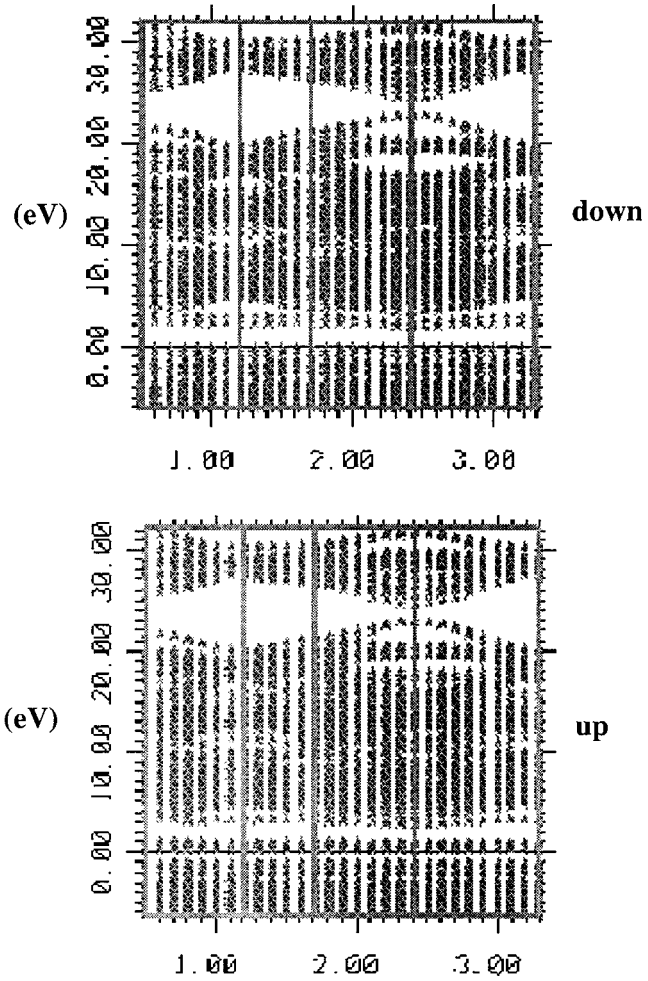

Figure 9. Band structures for T-shaped $[FeO_4]^{5-}$-doped $BaLiF_3$.

Table 1. α and β spin populations on Fe^{3+} and O^{2-} ions for the cross-shaped molecule.

	α electrons	β electrons	α electrons + β electrons	α electrons − β electrons
Fe^{3+}	14.057	11.547	25.604	2.510
O^{2-}	4.736	4.613	9.349	0.123

2.792 electrons and the $O1^{2-}$ and $O2^{2-}$ ions have lost 0.718 and 0.679 electrons respectively. One notes that the electron charge transferred from O1 atoms differs significantly from that transferred from O2 atoms.

The spin density distribution resulting from this electronic configuration is shown in figure 11 for two different orientations of the molecule. Again, a total ferromagnetic coupling between Fe and O atoms can be seen.

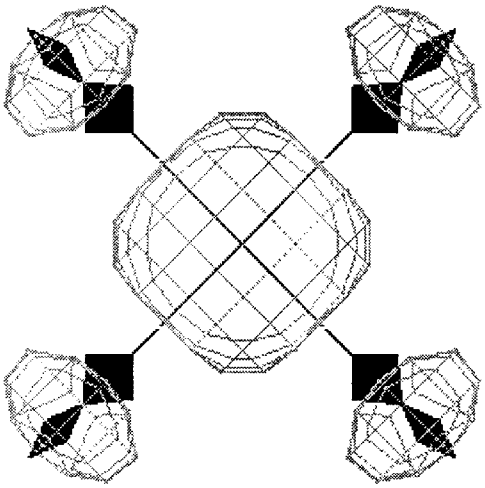

Figure 10. Spin density distribution for the cross-shaped $[FeO_4]^{5-}$ molecule. Level contour: 0.05 electron/bohr^3.

Table 2. α and β spin populations on Fe^{3+} and O^{2-} ions for the T-shaped molecule.

	α electrons	β electrons	α electrons + β electrons	α electrons − β electrons
Fe^{3+}	14.764	11.028	25.792	3.736
$O1^{2-}$	4.871	4.411	9.282	0.460
$O2^{2-}$	4.746	4.575	9.321	0.171

5. Discussion

Qualitatively, the theoretical approach used in our calculations of magnetic properties both on molecular and periodic models led to coherent results. Thus, a high spin value (HS = 5/2) was obtained for the complex with C_{2v} symmetry, and an intermediate spin value (IS = 3/2) was obtained for the complex with D_{4h} symmetry in both types of calculation. The atomic spin populations calculated for molecular and periodic models are in very good agreement. These theoretical results also agree with the experimental ones. The good agreement between cluster and periodic models, which include the $BaLiF_3$ matrix, shows that the experimentally observed phenomenon is purely local in nature.

The spin transition may be understood as a consequence of O jumpings under light or thermal excitation. The barrier deduced from our calculations is $E_{T\ shaped} - E_{cross\ shaped} = -1.56$ eV for periodic models and $E_{T\ shaped} - E_{cross\ shaped} = -1.96$ eV for molecular models. This value is much too high to account for thermal spin conversion and molecular bistability. However, these results must be regarded with caution as the calculations take into account neither the relaxation of the angular coordination of the C_{2v} group that necessarily occurs in the $BaLiF_3$ host lattice due to the low symmetry nor the influence of geometrical relaxations (bond lengths, bond angles) on the electronic properties. On the other hand, the electronic levels have to be dressed by the vibronic levels due to the lattice vibrations at finite temperature to discuss thermal spin conversion. The smearing out of the EPR lines of the C_{2v} group on heating can be seen as a consequence of the thermal excitation of vibronic levels. Reversibly, at low temperature these levels are empty and spin conversion is frozen or occurs slowly by

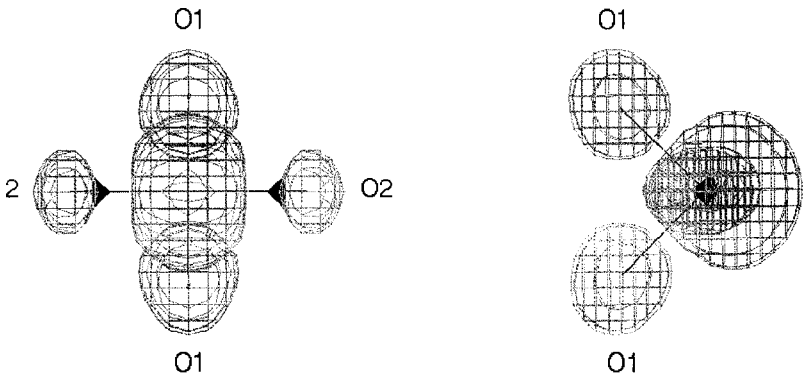

Figure 11. Spin density distribution for the T-shaped $[FeO_4]^{5-}$ molecule. Level contour: 0.05 electron/bohr^3.

tunnelling. Nevertheless, our qualitative results show the possibility of a low lying spin quartet for the ground state of Fe^{3+} surrounded by oxygen in a square plane configuration. As far as we know this has not been observed yet. It is worth noting that in the hypothetical crystal (figure 6(B)) the surroundings of Fe^{3+} are the same, up to the second atomic shell, as for the square plane site of copper in YBaCuO compounds.

6. Conclusions and perspectives

By using a local spin density approach as implemented in the DMol and ESOCS programs, we have investigated the electronic structure of both $[FeO_4]^{5-}$ molecules and $[FeO_4]^{5-}$-doped $BaLiF_3$ crystals. Two different $[FeO_4]^{5-}$ structures were studied: one with D_{4h} symmetry and another one with C_{2v} symmetry. Qualitatively, good agreement between theoretical and experimental results was found. Our calculations show that the $[FeO_4]^{5-}$molecule with D_{4h} symmetry has a quartet ground state and that the $[FeO_4]^{5-}$molecule with C_{2v} symmetry has a sextet ground state and that the former can be as deep as the latter. Thus, this computational study supports the hypothesis that $[FeO_4]^{5-}$ molecules may be the paramagnetic impurity originating the spin transition, which may be related to the structure transformation of these molecules as a consequence of O jumpings under light or thermal excitation. More definitive conclusions might be established by allowing geometrical relaxations for both molecular and crystalline models. Larger cluster models including the first shell of counterions and beyond should also improve the overall physical picture. Moreover, other theoretical approaches [17–19], such as ΔSCF and Slater transition state methods or other approximate functionals (e.g. Xalpha or BP86) that provide an almost quantitative description of the vertical excitation energies within the framework of DFT, may be used to perform a correct theoretical analysis of the optical properties of these systems, which would provide us with additional information about the validity of our models. Some calculations are in progress.

Acknowledgments

Isabel Lado Touriño would like to thank the Spanish Ministerio de Educación y Cultura for their financial support and María J Lado for technical assistance in the writing of this work.

References

[1] Cambi L and Cagnasso A 1931 *Atti Accad. Naz. Lincei* **13** 809
[2] Kahn O 1993 *Molecular Magnetism* (New York: VCH)
[3] Haddad M S, Federer W D, Lynch M W and Hendrickson D N 1980 *J. Am. Chem. Soc.* **102** 1468
[4] Haddad M S, Lynch M W, Federer W D and Hendrickson D N 1981 *Inorg. Chem.* **20** 123
[5] Haddad M S, Federer W D, Lynch M W and Hendrickson D N 1981 *Inorg. Chem.* **20** 131
[6] Decurtins S, Gütlich P, Köhler C P, Spiering H and Hauser A 1984 *Chem. Phys. Lett.* **105** 1
[7] Decurtins S, Gütlich P, Hasselbach K M, Hauser A and Spiering H 1985 *Inorg. Chem.* **24** 2174
[8] Ayad N 1995 *PhD Thesis* University of Maine
[9] Hohenberg P and Kohn W 1964 *Phys. Rev.* B **136** 864
[10] Delley B J 1990 *Chem. Phys.* **92** 508
[11] Vosko S J, Wilk L and Nusair M 1980 *Can. J. Phys.* **58** 1200
[12] Kuebler J and Eyert V 1991 *Electronic and Magnetic Properties of Metals and Ceramics* (Weinheim: VCH)
[13] Hedin L and Lundquist B I 1971 *J. Phys. C: Solid State Phys.* **4** 2064
[14] von Barth U and Hedin L 1972 *J. Phys. C: Solid State Phys.* **5** 1629
[15] Tressaud A 1985 *Inorganic Solid Fluorides, Chemistry and Physics* (New York: Academic)
[16] Fouassier C 1985 *Inorganic Solid Fluorides, Chemistry and Physics* (New York: Academic)
[17] Ziegler T 1995 *Can. J. Chem.* **73** 743
[18] Ziegler T 1994 *Chem. Rev.* **91** 651
[19] Slater J C 1971 *Adv. Quantum Chem.* **6** 1